IOP Publishing Smart Materials and Structures
Smart Mater. Struct. **23** (2014) 063001 (19pp) doi:10.1088/0964-1726/23/6/063001

Topical Review

A review on shape memory alloys with applications to morphing aircraft

S Barbarino[1], E I Saavedra Flores[2,5], R M Ajaj[3], I Dayyani[4] and M I Friswell[4]

[1] Mechanical, Aerospace and Nuclear Engineering, Rensselaer Polytechnic Institute, Troy, NY, USA
[2] Departamento de Ingeniería en Obras Civiles, Universidad de Santiago de Chile, Avenida Ecuador 3659, Estación Central, Santiago, Chile
[3] Aeronautics and Astronautics, University of Southampton, Southampton SO17 1BJ, UK
[4] College of Engineering, Swansea University, Singleton Park, Swansea SA2 8PP, UK

E-mail: erick.saavedra@usach.cl

Received 1 August 2013, revised 13 December 2013
Accepted for publication 7 January 2014
Published 10 April 2014

Abstract

Shape memory alloys (SMAs) are a unique class of metallic materials with the ability to recover their original shape at certain characteristic temperatures (shape memory effect), even under high applied loads and large inelastic deformations, or to undergo large strains without plastic deformation or failure (super-elasticity). In this review, we describe the main features of SMAs, their constitutive models and their properties. We also review the fatigue behavior of SMAs and some methods adopted to remove or reduce its undesirable effects. SMAs have been used in a wide variety of applications in different fields. In this review, we focus on the use of shape memory alloys in the context of morphing aircraft, with particular emphasis on variable twist and camber, and also on actuation bandwidth and reduction of power consumption. These applications prove particularly challenging because novel configurations are adopted to maximize integration and effectiveness of SMAs, which play the role of an actuator (using the shape memory effect), often combined with structural, load-carrying capabilities. Iterative and multi-disciplinary modeling is therefore necessary due to the fluid–structure interaction combined with the nonlinear behavior of SMAs.

Keywords: shape memory alloys, morphing aircraft, smart materials

(Some figures may appear in colour only in the online journal)

1. Introduction

Shape memory alloys (SMAs) are a type of material with the ability to recover their shape at certain characteristic temperatures. The material is able to return to its original geometry, even after reaching large inelastic deformations, near 10% strain (Huan 1998). Furthermore, an increase in temperature can result in shape recovery even under high applied loads, which results in high actuation energy densities (Kumar and Lagoudas 2008). In these cases, the actuation mechanism is controlled by the heating process and the recovery stress can be many times the initial stress required to pre-strain the alloy at a lower temperature. In addition, its typical mass density falls between that of aluminum and steel (about 5800 kg m^{-3}).

The first documentation of shape memory transformations dates back to the 1930s. At that time, Ölander (1932) noticed that the transformation of cadmium–gold alloy (Cd–Au) was reversible on the basis of metallurgical observations and resistivity changes. Greninger and Mooradian (1938) observed

[5] Author to whom any correspondence should be addressed.

Table 1. Alloys exhibiting a shape memory effect (Shimizu and Tadaki 1987, Lexcellent 2013, Hodgson*et al* 1990).

Alloy	Composition	Transformation range (°C)
Ag–Cd	44–49% Cd	−190 to −50
Au–Cd	46.5–50% Cd	30 to 100
Cu–Al–Ni	14–41.5% Al; 3–4.5% Ni	−140 to 100
Cu–Au–Zn	23–28% Au; 45–47% Zn	−190 to 40
Cu–Sn	15 at.% Sn	−120 to 30
Cu–Zn	38.5–41.5% Zn	−180 to −10
Cu–Zn–Al	3–8% Al	0 to 150
	4–6% Al; 22–28% Zn	Room temperature
In–Ti	18–23% Ti	60 to 100
Ni–Al	36–38% Al	−180 to 100
Ni–Ti	49–51% Ni	−50 to 110
Fe–Pd	30% Pd	−100
Fe–Pt	25% Pt	−130
Mn–Cu	5–35% Cu	−250 to 180
Fe–Mn–Si	32% Mn; 6% Si	−200 to 150

similar changes in brass (Cu–Zn) under thermal fluctuations. Later, Chang and Read (1951) coined for the first time the term 'shape memory effect' to describe the thermoelastic behavior of Cu–Zn. However, only at the beginning of the 1960s did the research on SMAs begin to gain popularity. During this period, Buehler *et al* (1963) found that nickel–titanium (NiTi) alloys, also called NiTiNOL, exhibited the shape memory effect too. As for many discoveries, this was due to chance and the deductive abilities of researchers (Kauffman and Mayo 1993). While investigating the behavior of NiTiNOL under fatigue resistance tests, Buehler and Wiley showed that wires made of this material returned to their original undeformed configuration when heated. A few years later, Buehler and Wiley were awarded a patent for the development of the NiTi alloy series (Buehler *et al* 1965).

Typically, NiTi alloy contains 49–57% nickel. The ideal composition of NiTiNOL can only vary between 38% and 50% titanium by weight, as only this composition possesses shape memory characteristics. NiTi alloy, often with some addition of copper (Cu), has proved to be one of the most interesting alloys to investigate. This material exhibits a great capacity to store a given 'shape', provided that the imposed strain does not exceed 8%. Table 1 reports some alloys that exhibit shape memory transformations.

There are multiple ways to produce an SMA. Generally these involve melting techniques using an electric arc or electron beam in a vacuum (Lin 1996). The molten alloy (at temperatures between 700 and 900 °C) is then shaped into rods by rotation or casting, and eventually into wires. There is also a process of cold production, in which the procedure is similar to the production of titanium. However, this process leads to different physical and mechanical properties for the alloy. Jackson *et al* (1972) addressed these issues in great detail. The study of the thermo-mechanical properties of SMAs and how they depend on the production process is of great interest in order to improve either the mechanical or the shape memory performance of the final alloy. Mahmud *et al* (2008) showed that it is possible to create NiTi materials with enlarged transformation intervals, either in stress or in temperature. They investigated a novel concept of partially annealing cold-worked near-equi-atomic NiTi alloys within a range of temperatures to create structurally graded matrices with continuously varying properties.

The shape recovery is associated with the existence of two different solid phases, each stable at a 'high' or 'low' temperature. The phase change produces a variation of the Young's modulus of between 2 and 4 times, with associated large variations in resistivity and release (or absorption) of latent heat. The temperatures at which the alloy recovers its shape can be modified by small changes in composition of the material and through heat treatments, to best fit the application requirements. The initial shape to which an SMA recovers can be assigned through a process of annealing, usually at temperatures of the order of 500 °C for the NiTi alloy.

In recent years, the availability of SMA materials with better characteristics and improved quality, together with reduced production costs, has allowed the development of an increasing number of products. These recent changes have promoted the spread of this type of material into different technological areas and the generation of new business opportunities and new research fields. Several applications can be found in aerospace, civil and mechanical engineering, and in military and medical devices, among many others. A wide selection can be found in Barbarino (2009).

Applications for morphing aircraft (Vocke III *et al* 2011, 2012) based on SMAs are of great scientific interest. The lifting surfaces of current aircraft are designed as a 'compromise' geometry that allows the aircraft to fly in a range of flight conditions, but the performance in each condition is likely to be sub-optimal. This is because the structure has to be rigid enough to support high cruise speeds and payloads, and is therefore optimized for a single condition (generally cruise for airplanes, hover for helicopters). The idea behind morphing is to overcome some of the limitations of current technology by adapting the geometry of lifting surfaces to pilot input and different flight conditions characterizing a typical mission profile. This approach, however, gives rise to an interesting paradox. The same structure has to endure the external aerodynamic loads without suffering appreciable deformations and, when needed, dramatically change its shape to fit the current flight condition. Shape memory alloys have been considered by several researchers as a viable solution to this challenge. Their mechanical properties allow for a straightforward integration within a larger structure, to complement the surrounding elements in carrying the aerodynamic loads. The shape memory effect, on the other hand, can be used on request to transition from passive to actuator-like behavior, and induce the desired geometry change. Nevertheless, SMAs can present some limitations, for instance, the long-term performance and reliability of SMA actuators, particularly when overheating and overstressing them over long periods of time, which may result in a considerable reduction of the fatigue life. Furthermore, SMAs have generally been considered to suffer from a slow response due to restrictions in heating and cooling (Teh 2008). In terms

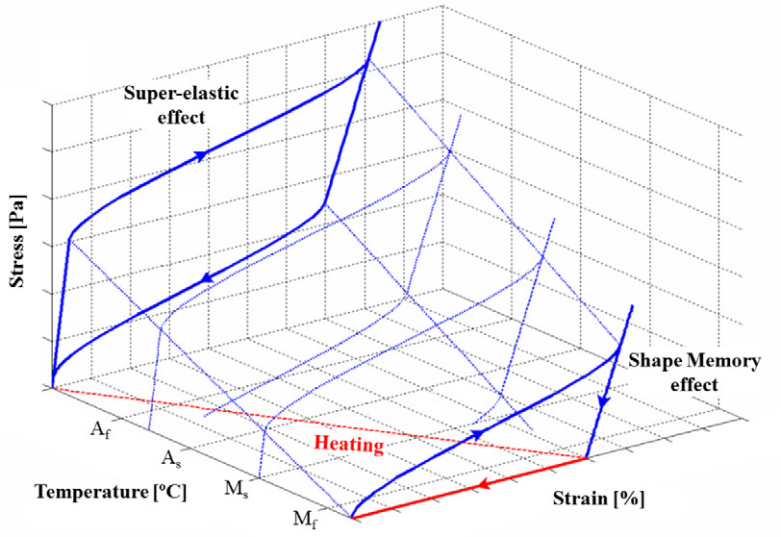

Figure 1. SMA stress–strain behavior. (a) The shape memory effect. (b) The pseudo-elastic effect.

of morphing aircraft, SMAs are mainly used for twist and camber morphing, and hence mainly for control authority. Therefore, it is vital to consider various measures to improve the actuator design to achieve the desired response. In addition, the need to reduce the overall power consumption is essential to maintain the system-level benefits of the morphing technology. Therefore, different strategies must be envisioned to optimize performance or power reduction according to the specific morphing application. Thus, before SMAs can be applied to morphing systems, the above concerns need to be addressed. This will represent the main contribution of the present article.

The article is organized as follows. Section 2 provides a general description of the thermo-mechanical behavior of SMAs. A review on the constitutive models of SMAs is presented in section 3. In section 4, the most relevant physical and mechanical properties of SMAs are reviewed, giving special attention to the fatigue phenomenon. Several applications of SMAs in the context of morphing aircraft are reviewed in section 5, including variable twist and camber. Actuation bandwidth and power consumption are also addressed in this section. Finally, section 6 summarizes our main conclusions.

2. Thermo-mechanical behavior and phase transformations

Shape memory alloys are characterized by a solid state phase transformation, in which both the starting phase (or parent phase, called austenite) and the final phase (or product phase, called martensite) are solid structures, although with different crystallographic arrangements (Kauffman and Mayo 1993). These two phases consist of a body-centered cubic structure for austenite, and a face-centered cubic structure for martensite. The transformation between these phases is known as the 'martensitic thermo-plastic transformation'. Due to the different crystalline structure, austenite behaves like many metals and has higher Young's modulus, whereas the martensite phase behaves more like an elastomer, with lower stiffness and a large 'plateau' in its stress–strain curve (resulting in the typical nonlinear behavior of SMA). The stable phase at any moment depends on the temperature, applied mechanical loads and thermo-mechanical history of the material.

The crystal structure of martensite is obtained from austenite following the application of a mechanical load or a decrease in temperature. Then, by heating or reducing the applied load, the austenite phase is recovered (Srinivasan and McFarland 1995, Brocca *et al* 2002). In stress-free conditions, some phase transformation temperatures (also called 'critical temperatures') can be identified as Ms, Mf, As, Af (M: martensite, A: austenite, s: start, f: final). For most SMAs, it results that $Mf < Ms < As < Af$.

By varying the temperature in the absence of applied loads, the phase of the material changes. The SMA composition is generally expressed in the literature in terms of the volume fraction of martensite (ξ). In particular, upon cooling, the material will start from a single phase composition of 100% austenite (temperature equal to or greater than Af and $\xi = 0$) to reach a condition of co-existence of both martensite and austenite in different proportions, and finally a 100% martensite phase (temperature at or below Mf and $\xi = 1$). When heating the alloy, the opposite process occurs. These transition temperatures increase with the applied load because more energy is required to deform the crystal structure.

As a result of this transformation, the observable macroscopic mechanical behavior of SMA materials can be separated into two categories, as follows.

(1) The 'shape memory' effect (SME) (figure 1(a)), in which an SMA specimen exhibits a large residual strain (apparently plastic) after being subjected to a load and then unloaded. After increasing the temperature, the alloy can completely recover this residual deformation.

(2) The 'pseudo-elastic' effect (figure 1(b)), in which the SMA specimen exhibits a very large deformation (apparently

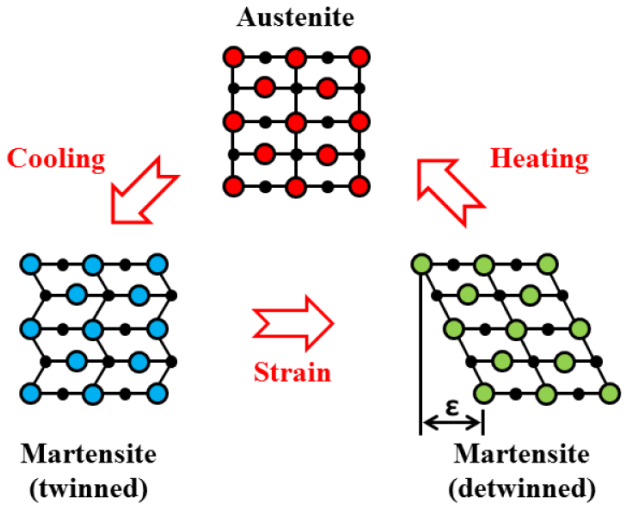

Figure 2. Microscopic phenomenology associated with the shape memory effect.

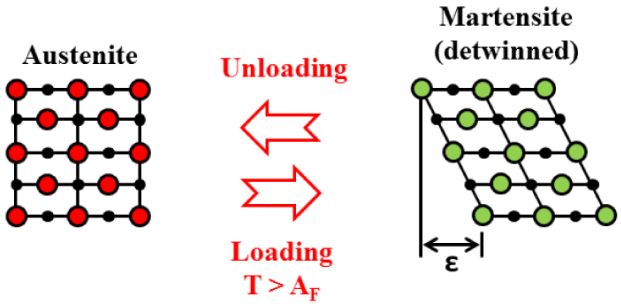

Figure 3. Microscopic phenomenology associated with the pseudo-elastic effect.

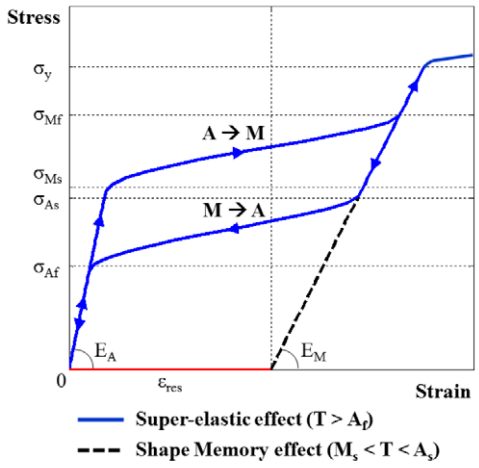

Figure 4. Typical SMA stress–strain diagram.

plastic) after being subjected to a load, which can then be completely recovered by means of a hysteretic loop when unloading.

The first property (SME) is particularly useful and is due to the specific crystalline structure of the martensite phase, which is the typical phase for an SMA at 'low' temperature. It consists of a dense arrangement of crystal planes placed with an opposite orientation and with very high relative mobility (resulting in low Young's modulus and good damping characteristics). When the material is loaded above the yield point in the martensite phase, instead of breaking the crystallographic ties, damaging its microstructure, the crystal planes gradually unfold the lattice, accommodating the strain without achieving significant atomic displacements. This phenomenon is called 'detwinning' (Chopra 2002) and is shown in figure 2.

The second property (pseudo-elasticity) of the martensitic transformation is related to the possibility of a phase transformation occurring by applying a suitable stress state under appropriate temperature conditions ($T >$ Af). The alloy can reach the same highly deformable crystalline structure during the application of an external force, directly going from the austenite phase to the deformed martensite phase. During loading, the material gradually forms the martensite structure which instantly deforms, without permanently damaging the crystal structure. Compared to the previous case, there is no twinned martensite phase (the martensite generated due to temperature decrease). However, since the phase transformation occurs in a temperature range where the martensite phase is not stable (for $T >$ Af the only stable phase is austenite), as soon as the external force is removed, the alloy reverts instantly to the parent phase, promoting an immediate shape recovery. The SMA immediately recovers its original shape and any large imposed deformation. Refer to figure 3 for details.

Both effects (SME and pseudo-elasticity) can be summarized in a single stress–strain diagram, as shown in figure 4, although for different temperatures.

The pseudo-elastic effect can be observed for an SMA tested at a temperature $T >$ Af, which is represented by the solid line. The SME is shown as a segmented line. Starting from a zero stress condition, the alloy is subjected to an applied stress. Initially the behavior is linear due to elasticity in the 100% austenite phase, with a Young's modulus equal to E_A. Then, the phase transition (from austenite to martensite) begins at the martensite start stress (σ_{Ms}). After the transition finishes, when the alloy is 100% martensite at the martensite finish stress (σ_{Mf}), the trend is linear again in the elastic range of the new phase (now the Young's modulus is E_M), stopping at the yielding limit (σ_y). In a typical application, the load reaches a level between σ_y and σ_{Mf}. Then unloading begins (always at a constant temperature $T >$ Af). Initially the same linear behavior associated with elastic unloading of martensite is followed, until the austenite start stress (σ_{As}) is reached. By decreasing the applied load below this stress (σ_{As}), the phase transition begins, and continues until reaching the 100% austenite phase, at the austenite finish stress (σ_{Af}). Further reduction in stress leads back to the initial condition in a linear elastic fashion.

On the other hand, if the loading–unloading process is conducted at a temperature Ms $< T <$ As, the shape memory effect takes place. Here, a similar trend with respect to the previous case is followed during the loading process. In this case the zero stress condition is reached with a residual strain in the alloy (ε_{res}). Only upon heating at a temperature $T >$ Af the material will recover this strain and its original shape again.

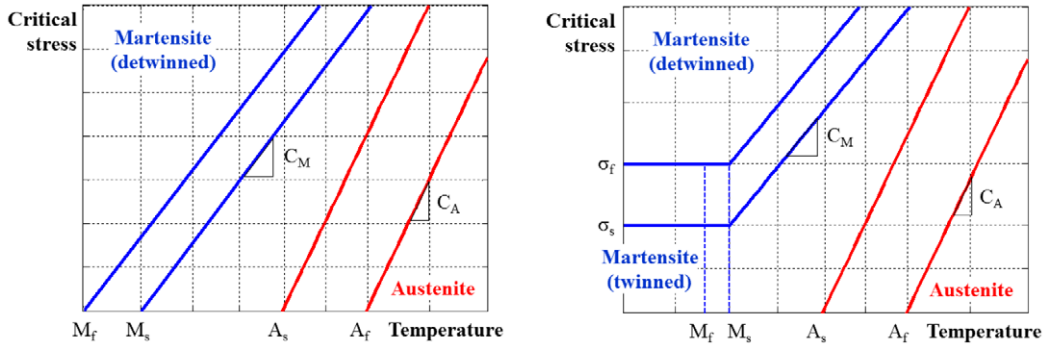

Figure 5. Critical stress–temperature profiles in constitutive models: (a) Tanaka; (b) Brinson.

Additionally, the shape memory effect can be of two different types:

(1) one-way shape memory;

(2) two-way shape memory.

The first category refers to SMA materials as hitherto discussed, for which a deformed shape must be imposed and upon thermal activation the initial configuration is attained. The second category, instead, relates to those materials that can 'remember' two shapes, each of which can be retrieved at a different temperature, without requiring an applied deformation. The two-way shape memory effect is usually achieved with SMAs that exhibit lower mechanical properties and after extensive training (loading–unloading). They also have lower performance as actuators (lower recovery stress when constrained). Two-way SMAs have been extensively studied. Refer, for instance, to Yu *et al* (2006), Huang and Toh (2000), Wada and Liu (2006).

Constitutive models for SMAs require some constants that can be obtained from the critical stress–temperature diagrams. Even if experiments show some slight nonlinearity, it is still possible to represent the trend of the critical stress as a linear function of the temperature. Figure 5 illustrates such transformation regions (Chopra 2002).

The regions marked with arrows are those in which the material exists in pure form. All other regions have a mixture of phases, and the exact content of the mixture depends on the thermo-mechanical history of the material. There are, however, differences in the definition of the material constants in different models. Both the Tanaka (1986) and the Liang and Rogers (1990) models assume a straight-line stress–temperature relationship, and Ms, Mf, As and Af correspond to the zero stress condition, as depicted in figure 5(a). For the non-zero stress condition, the critical temperatures will rise in a linear fashion. Usually these models also assume $C_A = C_M$ (curve slopes), with a constant value along all the temperature range. The stress–temperature relationship is somewhat different for the model proposed by Brinson (1990), and shown in figure 5(b). An additional region is present for the martensite twinned phase, which allows for modeling of the shape memory effect at low temperature. The constants Ms and Mf are defined as the temperature above which the application of stress does not cause a pure transformation from twinned to detwinned martensite. The critical stress σ_{cr}^{s} is the stress at which the transformation from twinned to detwinned martensite starts, and the critical stress σ_{cr}^{f} represents the stress where this transformation is nearly complete. These critical stresses are determined for a temperature below Ms and are considered independent of temperature. The strain at which detwinning is complete is usually referred to as ε_L (limit strain). Because of these differences, the interpretations of the transformation temperatures in the two models differ from each other. Therefore, when calculating these constants from the experimental critical points, the numerical values used by the Tanaka (1986) and Liang and Rogers (1990) models for Ms and Mf are obtained by extrapolating the martensite start and finish lines to zero stress, whereas those used by the Brinson model are obtained at the critical stresses σ_{cr}^{s} and σ_{cr}^{f}. These different values for the models must be used in order to obtain a fair comparison between these models and to match them to experimental observations.

If the coefficients are correctly identified from the experimental tests, all the considered models can predict the stress–strain behavior of the SMA in an acceptable way at temperatures higher than As (Prahlad and Chopra 2001a).

To determine the transformation temperatures (Ms, Mf, As and Af) of the SMA under the no stress condition, a Perkin–Elmer differential scanning calorimeter (DSC) is normally used (Chang 2006). This instrument uses the change in heat capacity of the material to determine the start and finish transformation temperatures. When the material undergoes phase transformation, it absorbs (or emits) a large amount of heat with a relatively small change of temperature, and the DSC captures such a change.

Frenzel *et al* (2010) obtained high-precision data on phase transformation temperatures in NiTi which included numerical expressions for the effect of Ni on Ms, Mf, As and Af. They showed that increasing the Ni content would decrease the width of thermal hysteresis and the heat of transformation, affecting the phase transition temperatures. More recently, Fabrizio and Pecoraro (2013) presented a model for shape memory alloy (AuZn) described by an intermediate pattern between a first and a second order phase transition.

3. Constitutive models for SMAs

Many constitutive models have been developed to describe the thermo-mechanical behavior of SMA materials. Some are based primarily on micro-mechanics, others on a combination of micro and macro-mechanics (SMA phenomenology), statistical mechanics or kinetic methods. The development of numerical methods such as finite element analysis (FEA) has led to a preference for constitutive models based on the description of the continuum (refer, for instance, to Saavedra Flores *et al* (2012), Saavedra Flores and Friswell (2012), and Saavedra Flores and Friswell (2013)). These models also use the typical engineering constants as parameters rather than quantities that are difficult to measure. Most of these macroscopic models have been developed for quasi-static loads only.

The first and most popular one-dimensional model is due to Tanaka (1986), and has already been mentioned in section 2. In this model, the second law of thermodynamics is written in terms of the Helmholtz free energy in variational form. Here, it is assumed that the mono-axial deformation ε, temperature T and volume fraction of martensite ξ are the only state variables. The constitutive equation is expressed as

$$(\sigma - \sigma_0) = E(\xi)(\varepsilon - \varepsilon_0) + \Theta(T - T_0) + \Omega(\xi)(\xi - \xi_0), \quad (1)$$

where the subscript 0 represents the initial condition. This equation shows that the total stress, $(\sigma - \sigma_0)$, is constituted by three quantities. These are the mechanical stress, $E(\xi)(\varepsilon - \varepsilon_0)$, the thermo-plastic stress, $\Theta(T - T_0)$, and the stress induced by the phase transformation, $\Omega(\xi)(\xi - \xi_0)$. Moreover, the Young's modulus E and the phase transformation coefficient Ω are functions of the martensite volume fraction ξ. These are usually expressed as

$$E(\xi) = E_A + \xi(E_M - E_A) \quad \text{and} \quad \Omega(\xi) = -\varepsilon_L E(\xi), \quad (2)$$

where ε_L is the maximum recoverable strain, and E_A and E_M represent the Young's moduli for the austenite and martensite phases, respectively. For the martensite volume fraction, Tanaka developed an evolutionary equation, determined by the dissipation potential, which depends on the stress σ and temperature T in an exponential fashion; that is,

A $\rightarrow$ M transformation (cooling),

$$\xi = 1 - \exp[a_M(M_S - T) + b_M\sigma], \quad (3)$$

M $\rightarrow$ A transformation (heating),

$$\xi = \exp[a_A(A_S - T) + b_A\sigma]. \quad (4)$$

Here, the material constants are defined as

$$a_A = \frac{\ln(0.01)}{(A_S - A_f)}, \qquad b_A = \frac{a_A}{C_A}, \qquad a_M = \frac{\ln(0.01)}{(M_S - M_f)} \quad \text{and} \quad b_M = \frac{a_M}{C_M}. \quad (5)$$

The adopted coefficients E, Θ and Ω, together with the parameters Ms, Mf, As, Af, C_A and C_M, are usually experimentally determined (Chopra 2002). We note that the transformation temperatures are measured for a zero stress condition. In particular, Ms and Mf can have different definitions and meanings according to the selected model.

Liang and Rogers (1990) presented a model based on Tanaka's constitutive equation. However, in their model a cosine function of temperature and stress is used to describe the volume fraction of martensite. Hence, the martensite volume fraction function is expressed as follows:

A $\rightarrow$ M transformation (cooling),

$$\xi = \frac{1 - \xi_0}{2}\cos[\alpha_M(T - M_F) + b_M\sigma] + \frac{1 + \xi_0}{2}, \quad (6)$$

M $\rightarrow$ A transformation (heating),

$$\xi = \frac{\xi_0}{2}\cos[\alpha_A(T - A_S) + b_A\sigma] + \frac{\xi_0}{2}, \quad (7)$$

where the constants are

$$\alpha_M = \frac{\pi}{M_S - M_f}, \qquad \alpha_A = \frac{\pi}{A_f - A_S}, \qquad b_M = -\frac{\alpha_M}{C_M} \quad \text{and} \quad b_A = -\frac{\alpha_A}{C_A}, \quad (8)$$

in which ξ_0 is the initial martensitic fraction. The cosine function argument can only assume a value between 0 and π. This implies that the phase transformation occurs only if the temperature is in an appropriate transformation range (or, similarly, if the stress is within a suitable stress range). That is,

A$\rightarrow$M transformation (cooling),

$$M_F \le T \le M_S \quad \text{and} \quad C_M(T - M_F) - \frac{\pi}{|b_M|} \le \sigma \le C_M(T - M_F), \quad (9)$$

M$\rightarrow$A transformation (heating),

$$A_S \le T \le A_F \quad \text{and} \quad C_A(T - A_S) - \frac{\pi}{|b_A|} \le \sigma \le C_A(T - A_S). \quad (10)$$

One of the major limitations of these models is that they only describe the stress-induced martensitic transformation (pseudo-elastic effect) and do not consider the transformation induced by the strain (shape memory effect). Therefore, they cannot be applied to model the detwinning of martensite which is responsible for the SME at low temperature.

Since the formulation of the original Tanaka model, it has been updated to cover the influence of the shape memory effect (Tobushi *et al* 1995, Lin *et al* 1995, Tanaka *et al* 1996, Tobushi *et al* 1996, Sittner *et al* 2000, Naito *et al* 2001). The primary update of the model has been carried out through the introduction of a new effect called the rhombohedral-phase transformation (RPT) or R-phase transformation. The RPT is a thermally reversible transformation that takes place at low strains and low temperatures, much like martensite detwinning. What makes it interesting is the low thermal hysteresis and cyclic stability, so that it allows the approximation of the stress–strain characteristic curve during unloading with the one during loading. The main disadvantage is the low attainable strain. At low temperatures (below As) RPT takes place, followed by the regular martensite transformation. At high temperatures (between As and Af) the RPT is

noticeable in the form of a small nonlinearity of the linear region of the pseudo-elastic curve. The RPT or R-phase effect is represented by a volume fraction coefficient η. Assuming the first cycle under zero stress/strain condition ($\eta = 0$, $\xi = 0$), an application of strain below 1% results in R-phase transformation ($\eta = 1, \xi = 0$). On heat activation, the R-phase is recovered. In all other cases this does not happen. Using this concept, the authors were able to correlate predictions with test data especially at low temperatures. Naito *et al* (2001) and Sittner *et al* (2000) represented the RPT and martensite transformation in a unified way using an energy function, with appropriate 'switching functions' to handle different transformations.

In addition to the use of SMA wires under uniaxial loading as actuation elements, SMA rods and tubes have also been used for twist actuation. The principle of operation is the same as in the case of SMA wires. Here, the rod (or tube) is first pre-twisted and then tends to recover its original, untwisted state when heat activated.

To overcome the limitation of not representing the stress-induced martensite, Brinson (1990) developed a constitutive model that separates the volume fraction of martensite into two parts. One is stress induced (often referred to in the literature as stress-induced martensite, SIM) and one is induced by temperature. The first part characterizes the amount of detwinned martensite present in the alloy (stress-induced), while the second is the fraction of twinned martensite, present after the reversible phase transformation from austenite. To model both the shape memory and pseudo-elastic effects, the coefficients of the constitutive equation are considered to be variable. That is,

$$\sigma - \sigma_0 = E(\xi)\varepsilon - E(\xi_0)\varepsilon_0 + \Omega(\xi)\xi_S - \Omega(\xi_0)\xi_{S0} + \Theta(T - T_0), \tag{11}$$

where the martensite volume fraction is $\xi = \xi_S + \xi_T$, with ξ_S the portion of detwinned (or stress preferred) martensite present at low temperature and ξ_T the portion of twinned (or randomly oriented) martensite that comes from the reversible thermal phase transformation from austenite.

Another constitutive model has been proposed by Boyd and Lagoudas (1996a, 1996b), which is based on the free energy and dissipation potential. This model is derived from the Gibbs free energy (determined by summing the free energy of each phase of shape memory materials plus the free energy of mixing) instead of the Helmholtz free energy, as used in the Tanaka model. This model can handle three-dimensional effects and non-proportional loads. A constitutive relation satisfying the second law of thermodynamics is then developed. The total strain consists of two parts: the mechanical strain ε_{ij} and the transformation strain ε_{ij}^{tr}, which is a function of the martensite volume fraction. That is,

$$\sigma_{ij} = C_{ijkl}[\varepsilon_{kl} - \varepsilon_{kl}^{tr} - \alpha_{kl}(T - T_0)]. \tag{12}$$

Peng *et al* (2005) proposed a two-phase mixture model incorporating the conventional theory of plasticity. Matsuzaki *et al* (2001) developed a general one-dimensional thermo-mechanical model taking into account the effects of energy dissipation, latent heat and heat transfer during the phase transformation. Heintze (2004) developed a computationally efficient free energy model. A first implementation was based on a stochastic homogenization procedure and provided a very accurate description of the observed phenomena, but required very high computation times. Auricchio and Reali (2008), Auricchio *et al* (2007, 2008, 2009) addressed some three-dimensional models, considering the isothermal stress-induced transformation in shape memory polycrystalline materials and the presence of permanent inelasticity.

Recent works have highlighted some limitations of phenomenological models. Elahinia and Ahmadian (2005a, 2005b) noted that in certain circumstances, combining contemporary variation of the applied stress and temperature (which may be a result of the physics of the problem), the model predictions do not correlate with experimental data. This can be attributed to the dependence of the critical temperatures on the applied stress and the assumption that the phase transformation is only possible between appropriate critical temperatures in the direction of the thermal cycle (and not otherwise).

Due to the complexity in the reproduction of the SMA phenomenology, some studies have focused on the adoption of reinforcement learning (Haag *et al* 2005, Valasek *et al* 2005, 2008, Kirkpatrick and Valasek 2008). This is a form of machine learning that utilizes the interaction with multiple situations many times in order to discover the optimal path that must be taken to reach the pre-determined goal.

Kadkhodaei *et al* (2007a) presented a one-dimensional coupled thermo-mechanical model of SMAs under non-quasi-static loading by defining a Helmholtz free energy function consisting of strain energy, thermal energy, and the energy of phase transformation. Kadkhodaei *et al* (2007b, 2008) presented a three-dimensional microplane constitutive model which included the statically constrained formulation with volumetric–deviatoric split for the shape memory alloys. They described the shear stress within each microplane by the component of resultant shear on the plane and then used one-dimensional stress–strain laws by considering proper adjustments between the macroscopic and the microscopic quantities. Moreover, they showed the interaction between the stress components and the deviation from normality in the case of non-proportional loadings. Kan and Kang (2010) proposed a new cyclic constitutive model in a framework of generalized plasticity to predict the uniaxial transformation ratcheting at room temperature. They considered the dependence of transformation ratcheting on the applied stress levels and the phase transformation hardening behavior of the NiTi alloy. Their model accounted for the evolutions of residual induced-martensite and transformation-induced plastic strain during the stress-controlled cyclic loading by introducing the accumulated induced-martensite volume fraction as an internal variable. Arghavani *et al* (2010) presented a phenomenological constitutive model based on scalar and tensorial internal variables for shape memory alloys within the framework of irreversible thermodynamics. Chemisky *et al* (2011) proposed a three-dimensional model for shape memory alloy to account for several aspects of the thermo-mechanical behavior of SMAs. Their model was focused on the behavior

Table 2. Variability of SMA properties (Srinivasan and McFarland 1995, Huang 2002, Otsuka and Wayman 1998, Duerig and Pelton 1994, Gerstner 2002).

	NiTi	Cu–Zn–Al	Cu–Al–Ni
Physical properties			
Grain size (μm)	1–100	50–150	25–100
Density (g m^{-3})	6.4	6.45	7.64
Thermal expansion coefficient (10^{-6} K^{-1})	6.6–11	17	17
Resistivity ($\mu\Omega$ cm)	80–100	8.5–9.7	11–13
Damping capacity (SDC%)	15–20	30–85	10–20
Thermal conductivity (W m^{-1} K^{-1})	10	120	30–43
Normal number of thermal cycles	$>10^5$	$>10^4$	$>5 \times 10^3$
Melting temperature (K)	1573	1223–1293	1273–1323
Heat capacity (J kg^{-1} K^{-1})	390	400	373–574
Mechanical properties			
Normal working stress (GPa)	0.5–0.9	0.4–0.7	0.3–0.6
Fatigue strength ($N = 10^6$) (GPa)	0.35	0.27	0.35
Young's modulus (GPa) (parent phase)	83	72	85
Young's modulus (GPa) (martensite)	34	70	80
Yield strength (GPa) (parent phase)	0.69	0.35	0.4
Yield strength (GPa) (martensite)	0.07–0.150	0.08	0.13
Ultimate tensile strength (GPa)	0.9	0.6	0.5–0.8
Transformation properties			
Heat of transformation (J mole^{-1}) (martensite)	295	160–440	310–470
Heat of transformation (J mole^{-1}) (R-phase)	55	—	—
Hysteresis (K) (martensite)	30–40	10–25	15–20
Hysteresis (K) (R-phase)	2–5	—	—
Recoverable strain (%) (one-way martensite)	8	4	4
Recoverable strain (%) (one-way R-phase)	0.5–1	—	—
Recoverable strain (%) (two-way martensite)	3	2	2

at low stress level and a unique mechanism. They introduced the accommodation of twins present in NiTi to explain the change of apparent modulus between austenite and self-accommodated martensite. They showed the applicability of their model for describing the non-proportional loading in the case of transformation, orientation or the combination of both mechanisms. Morin *et al* (2011) extended the Zaki–Moumni model (2007) of SMAs to account for the thermo-mechanical coupling. They modified the expression of the Helmholtz free energy in order to derive the heat equation in accordance with the principles of thermodynamics. The thermo-mechanical coupling allowed them to reproduce the strain rate dependence of the mechanical response. More recently, based on the crystal plasticity, Yu *et al* (2013) constructed a new micromechanical constitutive model to describe the cyclic accumulation of plastic strain in polycrystalline NiTi shape memory alloy during the thermo-mechanical cyclic loading. They considered both the transformation-induced plasticity and the residual martensite phase as the main contributions to the plastic strain and formulated the Helmholtz free energy for a representative volume element of single crystal. Mehrabi and Kadkhodaei (2013) used the microplane theory to model the 3D phenomenological behavior of shape memory alloys. They assumed that the transformation is the only source of inelastic strain in a 1D constitutive law for any generic plane passing through a material point. Furthermore, by use of homogenization technique they generalized the 1D equation and derived 3D constitutive equations.

Finally, a variety of implementations of some of these models can be found in the literature, taking advantage of different commercial finite element solvers: ABAQUS (Han and Lu 2006, Richter *et al* 2009, Chemisky *et al* 2008, Gong *et al* 2004), FEMLAB, now COMSOL Multi-physics (Li and Seelecke 2007, Shrivastava 2006, Collet 2008, Thiebaud *et al* 2005, Yang and Seelecke 2008), ANSYS (Terriault *et al* 2006, Sreekumar *et al* 2008), and MSC/Marc (Saeedvafa 2002).

4. SMA properties and fatigue

SMA properties can have a wide variability according to the chemical compositions and heat treatments to which the alloy has been subjected. Typical properties for the most widely available SMAs, such as NiTi, Cu–Zn–Al and Cu–Al–Ni alloys, are summarized in table 2 (Srinivasan and McFarland 1995).

Among all shape memory alloys, NiTi alloys deserve special consideration. Ever since their discovery, these materials have received particular attention for their higher thermo-mechanical properties and lower production costs (when compared, for instance, to the first Ag–Cd alloy) and, to date, are among the most popular. Table 3 reports the main features of

Table 3. Typical properties for NiTi alloys (Johnson Matthey Inc. 2013, Jani*et al* 2014, Huang 2002, Kumar 2000, Fugazza 2005, Shuai*et al* 2009).

Transformation temperatures and strains	
Transformation temperature range	−200[a]–100 °C
Transformation enthalpy	0.47–0.62 kJ kg^{-1} K^{-1}
Transformation strains: up to 1 cycle	up to 8%
Transformation strains: up to 100 cycles	up to 5%
Transformation strains: up to 100 000 cycles	up to 3%
Transformation strains: above 100 000 cycles	ca. 2%
Thermal hysteresis[b]	30–80 °C
Latent heat of transformation	40 cal/g-atom
Physical properties	
Melting point	ca. 1310 °C
Density	6.45–6.5 kg dm^{-3}
Thermal conductivity of the martensite	ca. 9 W m^{-1} K^{-1}
Thermal conductivity of the austensite	ca. 18 W m^{-1} K^{-1}
Resistivity austenite	∼100 $\mu\Omega$ cm
Resistivity martensite	∼70 $\mu\Omega$ cm
Corrosion properties and biocompatibility	Excellent
Specific heat	0.20 cal g^{-1} $°C^{-1}$
Magnetic permeability	<1.002
Magnetic susceptibility	3.0e + 6 emu g^{-1}
Mechanical properties	
Young's modulus of the austenite	ca. 70–80 GPa
Young's modulus of the martensite	ca. 23–41 GPa
Poisson's ratio	0.33
Ultimate tensile strength (coldworked condition)	up to 1.900 MPa
Ultimate tensile strength (fully annealed condition)	ca. 900 MPa
Elongation to fracture of the austenite	1–20%
Elongation to fracture of the martensite	up to 60%
Plateau stress martensite	70–200 MPa
Plateau stress austenite	200–650 MPa
Yield stress austenite	550–700 MPa
Yield stress martensite Transverse contraction factor (Poisson's ratio)	∼100 MPa 0.33
Tensile strain (fully annealed)	20–60%
Tensile strain (coldworked)	5–20%
Melting, casting and composition control	Difficult
Forming (rolling, extrusion)	Difficult
Hot workability	Reasonable
Cold workability	Fair
Machinability	Difficult

[a] Low transformation temperatures can be attained by increasing the amount of nickel; however, this makes the material extremely brittle.
[b] The hysteresis is evaluated on complete load–unload cycles; it reduces for partial cycles.

a typical NiTi alloy. These values have been obtained from Johnson Matthey Inc. (2013).

One of the main problems that may affect the mechanical and physical properties of SMAs is fatigue, particularly when exposed to overheating and overstressing over long periods of time. In general, the long-term performance and fatigue behavior of SMAs depend on the material processing (for instance, fabrication process and heat treatment), the type of loading conditions (maximum temperature, stress, strain, environment, etc) and the transformation cycles achieved, among others. In most cases, SMA applications undergo a large number of transformation cycles by repeating a thermo-mechanical loading path, which may result in microstructural damage and, therefore, in low cycle fatigue (Kumar and Lagoudas 2008).

The fatigue behavior of SMAs can be induced by mechanically cycling the material between two stress or strain levels along a given loading path (Miller and Lagoudas 2000). In such a case, if the applied strain or stress level remains within the elastic regime, the fatigue life can be extended to as high as 10 million cycles (Kumar and Lagoudas 2008). On the contrary, if the SMA is cycled at high levels of load, through detwinning

or stress-induced martensitic transformation, the fatigue life may be reduced to the order of thousands of cycles (Tobushi *et al* 1997).

The fatigue behavior of SMAs can also be produced by thermally-induced transformation cycles. On undergoing this type of thermal cycles, the fatigue behavior depends on the amount of transformation strain and stress level. A partial transformation may cause a significant extension of fatigue life (Miller and Lagoudas 2000, Bertacchini *et al* 2003). For instance, in wires of NiTiCu under a fixed stress level of 200 MPa, an extension of the fatigue life by a factor of approximately seven has been reported for a partial martensitic transformation (Kumar and Lagoudas 2008).

Further investigations addressed the issue of fatigue in SMAs, and particularly of removal or reduction of its undesirable effects. Gall *et al* (2008) observed that the precipitate size and the crystallographic orientation in SMAs are also factors that may affect the fatigue life. These authors studied the fatigue performance of hot-rolled and cold-drawn NiTi bars. They obtained fatigue threshold values some five times smaller for the cold-drawn bars than the hot-rolled material. This difference was attributed to the significant residual stresses in the cold-drawn material, which amplify fatigue susceptibility despite superior measured monotonic properties.

Advancement in the development and processing of materials may also reduce degradation and fatigue. For instance, Flexinol (the trade name of NiTi SMAs manufactured by Dynalloy Inc.) wires have been trained to exhibit the shape memory effect over millions of cycles without fatigue (Teh 2008). These results were obtained for 0.1 mm diameter wires undergoing working strains limited to 4%, with an austenite finish temperature of 90 °C.

In addition, high annealing temperatures and a chemically active environment may lead to corrosion and therefore to crack nucleation and growth, resulting in a reduction of the fatigue life of SMAs (Tobushi *et al* 1997, Bertacchini *et al* 2003). Furthermore, one of the most common methods in actuation is electrical heating. Although the application of large electrical currents may speed up the actuation, this can also overheat and damage the SMA actuator (Teh 2008).

Eggeler *et al* (2004) discussed four cases of fatigue in NiTi shape memory alloys: the evolution of the stress–strain hysteresis in the low cycle pull–pull fatigue of pseudo-elastic NiTi wires, the bending–rotation fatigue rupture of pseudo-elastic NiTi wires, strain localization during the stress-induced formation of martensite and generic features of functional fatigue in NiTi shape memory actuator springs. They showed that the microstructure was important in governing the stability of the stress–strain hysteresis during strain-controlled fatigue.

Scirè Mammano and Dragoni (2011, 2013) investigated four test conditions on SMAs under cyclic thermal activation: constant-stress, constant-strain, constant-stress with limited maximum strain and linear stress–strain variation with limited maximum strain. These authors found an increase of the fatigue life in the constant-stress condition with limited maximum strain when compared with the regular constant-stress tests. They showed that exposure to constant-strain conditions was detrimental to the fatigue life. It was also shown that the linear stress–strain variation with a limited strain of 4% resulted in a marked reduction of the fatigue limit with respect to the constant-stress tests.

Matheus *et al* (2011) evaluated two NiTi wires with different carbon and oxygen contents in terms of mechanical resistance to rotary bending fatigue under different parameters of strain amplitude and rotational speed. They showed that the surface quality of the wire was related to the resistance to fatigue. They also found that a smaller carbon content results in better performance to fracture.

Takeda *et al* (2013) implanted high energy nitrogen ions on the surface of TiNi wires and discussed their influence on the bending fatigue properties. They showed that the thermo-mechanical properties change, resulting in a long fatigue life.

5. SMAs in morphing aircraft applications

Recently, the use of shape memory alloys has gained a wide interest in the field of morphing aircraft. The philosophy of aircraft designers is to maximize the synergy of the system by maximizing its functionalities. SMAs are ideal candidates for such a philosophy as they can take the role of actuators and at the same time act as load carrying members.

Departing from the conventional rigid, wing-box-like structures, researchers have designed novel structural configurations which maximize the integration and effectiveness of shape memory alloys to achieve the morphing goal. They have been faced with the two-fold challenge of modeling the nonlinear thermo-mechanical behavior of the shape memory alloy and its interaction with the surrounding unconventional structure subject to external loads. Modeling of the fluid–structure interaction can already be challenging and computationally expensive by itself. The study of unconventional structures may require specific tools or finite element solvers. The analysis of a complete structural assembly implementing SMAs would require an iterative multi-disciplinary approach, with a combined thermo–aero-mechanical analysis.

The correct estimate of the mechanical behavior of the SMA and its stress–strain state as a function of external loads and temperature is crucial to the design of a morphing aircraft application. As shown in this article, there are multiple models for shape memory alloys developed in the literature, each addressing specific loading conditions and presenting some limitations. In fact, no general model exists to date for SMAs which: (1) is capable of predicting their behavior under any complex or combined loading, (2) can be used for a generic structural element type, (3) is formalized based on easily measurable engineering quantities and (4) can be converted to a tool or interfaced with standard design tools widely adopted by researchers and engineers.

The lack of a 'final' SMA model, as demonstrated by the on-going theoretical and experimental studies within the international community, has constrained the type and complexity of structural configurations developed in morphing aircraft, which are usually based on simple SMA wires or beams. Often in-house tools and algorithms are used by researchers to analyze and design the specific applications.

This lack of generic tools, in turn, has negatively affected the interest from the industry side.

Nonetheless, a variety of numerical and experimental studies dealing with SMAs for morphing applications can be found in the literature. Even flying test beds with SMAs have been developed and tested. It should be noted that the majority of studies have focused on UAVs and rotorcraft. A comprehensive review of the morphing aircraft literature by Barbarino *et al* (2011) shows that SMAs have been mainly used for twist and camber morphing. Large planiform morphing such as span, chord, and sweep are not feasible with SMAs due to their relatively low strain and high density. Several works will be discussed herein.

5.1. SMA actuation of twist and rigid-body rotation

The Smart Wing program of DARPA, AFRL, NASA and Northrop Grumman (Martin *et al* 1998, Kudva and Carpenter 2000) realized an unmanned combat air vehicle (UCAV) by integrating SMAs within a morphing wing. This experimental study implemented both SMA torque tubes for wing twist and flexible leading and trailing edges actuated by SMA wires. The SMA torque rods were connected to a torque transmission rod to transfer the loads to the wing box. Barrett *et al* (2001) introduced a pitch active SMA wing UAV with a 2 m span. This flight tested fixed wing aircraft had SMA wires that changed the pitch of the main wings. The SMAs caused a rigid-body rotation of the wings. Nam *et al* (2002) used SMA spars to replace the mechanically actuated variable stiffness spar (VSS) concept to enhance the aeroelastic performance of the wing. They adopted active property tuning (APT) where the SMA was embedded without plastic elongation. Therefore, no internal stresses are induced, and the SMA varies its stiffness. A wing model based on the F-16 demonstrated that the SMA spar can further amplify the aeroelastic forces and significantly enhance roll performance compared to the traditional VSS concept. Furthermore, locating the SMA spar towards the trailing edge maximized the improvement in roll rate in comparison to the traditional VSS concept (61%).

Elzey *et al* (2003) developed an antagonistic shape morphing structural actuator, comprising of a cellular flexible core sandwiched between SMA face sheets that induced curvature upon heating. The core was an assembly of modular elements able to rotate relative to one another (vertebrate structure); hence the actuator could reverse its shape without any bias mechanism to provide the elastic restoring force. A prototype wing was built in which the vertebrate actuators were incorporated as ribs. The wing also twisted by asymmetric actuation of its two SMA actuated vertebrate beams. Similarly, Sofla *et al* (2008) used antagonistic flexural cells (AFCs) to create two-way SMA flexural actuators using a one-way shape memory effect. The cells provided four distinct positions for each segment of the actuator, and two of the positions required no external energy to be maintained. These actuators could control the twist of wing sections if they were incorporated as ribs and were actuated asymmetrically.

Lv *et al* (2009) developed an SMA torsion actuator based on NiTi wires and a thin-walled tube for an adaptive wing demonstration system. The angle of attack of the wing could be changed continuously up to 15° in 1 s. A novel smart wing rib with swing angles up to ±10° was investigated.

SMAs have also been applied for wing twist on helicopter rotor blades. Prahlad and Chopra (2001b) developed and tested a torsional SMA actuator to alter the twist distribution for a tiltrotor blade between hover and forward flight. The design of the actuator (torque tube) was optimized as a function of heat transfer, temperature and actuation recovery torque. The effect of heat treatment on the tuning of the actuation characteristics of the SMA tube was also investigated, and thermoelectric modules were used to release excess heat through the blade surface to improve the cooling and reduce the actuation time. Chandra (2001) developed a method to induce twisting deformation in a solid-section composite beam using SMA bender elements. Bending–torsion coupled graphite-epoxy composite beams with Teflon inserts were built using an autoclave molding technique and the Teflon inserts were replaced by SMA bender elements. The composite beams were actuated by heating the SMA via electrical resistive heating, and the bending and twisting deformation was measured using a laser system. Such beams with SMA elements can be used as spars in rotor blades to induce twist.

The goal of the reconfigurable rotor blade (RRB) program funded by NAVAIR was to demonstrate the potential to improve rotorcraft performance by optimizing the configuration of major structures in flight (Bushnell *et al* 2008, Arbogast *et al* 2008). The SMA actuation system employed 55-NiTiNOL (Ni-55Ti) rotary actuators integrated as structural elements in a quarter scale rotor blade to control twist. A passive torque tube transmitted the torque from the actuator assembly near the blade root to the tip of the blade causing the blade to twist. A lightweight spring mechanism, the strain energy shuttle, provided an energy storage element between the SMA actuator and the passive torque tube, and halved the actuator system weight (Calkins *et al* 2008). The actuator was tested in 2007 using a 1/4 scale three blade hub assembly mounted on the Boeing advanced rotor test stand. The wind tunnel test was a high-fidelity assessment of the SMA actuator (Ruggeri *et al* 2008) and represents one of the first attempts to produce a high-torque SMA actuator for the rotor environment. The actuator provided approximately 250 twist transitions during 75 h of testing with no loss of performance or operational anomalies.

5.2. Shape memory alloy and similar actuation for camber

Roglin *et al* (1994) and Roglin and Hanagud (1996) presented an adaptive airfoil that used a shape memory alloy actuator mechanism to actively change the camber of an airfoil for a remotely piloted helicopter. The airfoil concept was demonstrated on a remote control helicopter with active camber airfoils. Embedded SMA wires were used to bend the trailing edge of the rotor blade to morph the airfoil camber. This camber morphing was then used to replace the collective pitch control of the helicopter. The change in rotor thrust response due to the SMA was linearized by a controller which accepted the signal from the radio receiver and applied the

heating required to deform the SMA. Due to the low frequency response of the system, only steady collective control was attempted.

Kudva *et al* (1996a, 1996b), Kudva and Carpenter (2000) and Kudva (2001) worked on SMA applications for a morphing wing. Kudva (2004) documented the DARPA, AFRL, NASA, Northrop Grumman Smart Wing program as it evolved since its inception in 1995. The program aimed to realize a UCAV and considered the application of smart materials to improve the performance of military aircraft. The project consisted of two phases and both phases had experiments with SMAs. The program utilized an SMA to contour the trailing edge control surfaces, and SMA torque tubes to vary the wing twist. Early efforts highlighted the bandwidth issues of SMAs. During the second phase, a 30% scaled design was tested over a range of Mach 0.3–0.8, and resulted in significance performance improvements (increased lift, and a roll rate of 80° s^{-1}). From wind tunnel tests, an improvement between 8% and 12% in lift and roll control over a traditional wing was observed. A wing twist of up to 5° was attained, together with a deflection of up to 4.5° for the leading edge and 15° for the trailing edge. Kudva (2004) mentioned that the 'Smart Wing's control surfaces showed no degradation in performance during the 3 weeks of wind tunnel testing'. Sanders *et al* (2004) presented the wind tunnel results obtained during phase 1 and phase 2 of the Smart Wing program.

Chopra (2001, 2002) and Epps and Chopra (2001) systematically investigated the development of an SMA actuated trailing edge tab for in-flight blade tracking. This wing section was tested in an open-jet wind tunnel, and tab deflections of the order of 20° were obtained. Singh and Chopra (2002) improved this design and successfully tested it in the wind tunnel with repeatable open-loop and closed-loop performance. Beauchamp and Nedderman (2001) patented a design with shape memory alloys that were embedded within a control surface on the blade of a wind turbine.

Strelec *et al* (2003) utilized a global optimization method that incorporated a coupled structural, thermal, and aerodynamic analysis to determine the necessary placement of the SMA wire actuators within a compliant wing. A genetic algorithm (GA) was chosen as the optimization tool to efficiently converge to a design solution. The GA used was a hybrid version with global search and optimization capabilities augmented by the simplex method with selective line search as a local search technique. The lift-to-drag ratio was maximized for a reconfigured airfoil shape at subsonic flow conditions. A wind tunnel model of the reconfigurable wing was fabricated based on the design optimization to verify the predicted structural and aerodynamic response. Wind tunnel tests indicated an increase in lift for a given flow velocity and angle of attack by activating the SMA wire.

Alasty *et al* (2004) studied the effect of a variable shape wing applied to an ultra-light aircraft, in order to improve aerodynamic efficiency and flight control. Given the size (less than a meter of wingspan) and the low weight of this aircraft, SMAs were more appropriate than traditional actuators thanks to their high strength, low weight, and reduced footprint. The structure was made of balsa wood with nylon sticks; the wings were composed of two parts, a rigid front element and a deformable rear. SMA actuators were used in pairs, and so each wire acted in opposition to the other; this concept is often found in the literature and is called the antagonistic configuration.

Benavides and Correa (2004) realized a wing section based on the symmetric Gottingen 776 airfoil, with a deformable trailing edge actuated by SMA wires. Wind tunnel tests verified the improvement in terms of lift-to-drag ratio and lift coefficient of this solution with respect to a traditional one. The wing section used six NiTiNOL wires that could pull, upon electrical activation, the upper part of the wing trailing edge downward. In a different application, Madden *et al* (2004) varied the camber of a marine propeller using Polypyrrole actuators. These actuators behave like artificial muscle by extending and contracting with voltage, and promise to provide the actuation forces and strains required to change the camber of the propeller foils. Two Polypyrrole actuators operated as an antagonistic pair to operate tendons attached to the trailing edge of the foil. In order to achieve the desired degree of strain two concepts were compared: the two actuators were arranged in the form of a bimetallic strip so as to complement each other, or a lever arrangement was used. Both of these methods were examined by experimental testing.

Mirone (2007) and Mirone and Pellegrino (2009) investigated the ability of a wing to modify its cross-section (assuming the shape of two different airfoils) and the possibility of deflecting the profiles near the trailing edge in order to obtain hingeless control surfaces. One-way shape memory alloy wires coupled to springs provided the actuation. The points to be actuated along the profiles and the displacements to be imposed were selected so that they satisfactorily approximated the change from one airfoil to the other and resulted in an adequate deflection of the control surface. The actuators and their performance were designed to guarantee adequate wing stiffness in order to prevent excessive deformations and undesired airfoil shape variations due to aerodynamic loads. Two prototypes were realized, incorporating the variable airfoil and the hingeless aileron features respectively, and the verification of their shapes in both the actuated and non-actuated states. The comparison of the real wing profiles with the theoretical airfoil coordinates showed a good performance of the actuation system. A significant trailing edge displacement, close to 10% of the wing chord, was achieved in the experimental tests.

Brailovski *et al* (2008) considered a morphing wing concept designed for subsonic cruise flight conditions combining three principal subsystems: a flexible skin, a rigid interior structure and an actuator group located inside the wing box. Using a weighted evaluation of the aerodynamic and mechanical performances in the framework of a multi-criterion optimization procedure, an adaptive structure consisting of a 4-ply flexible skin powered by two individually controlled actuators was designed. The forces these actuators must provide in order to fit target wing profiles are calculated for a given flexible structure and given flight conditions. Each actuator includes linear SMA active elements with one extremity connected, through a cam transmission system, to the flexible skins and the other extremity connected to the rigid structure of the wing

through a bias spring. To meet the functional requirements of the application, the geometry (length and cross-section) of the SMA active elements and the bias spring characteristics are calculated.

Peel *et al* (2008, 2009) constructed a variable camber morphing wing using elastomeric composites as the internal actuators. The skin of the wing was a carbon fiber and polyurethane elastomeric composite that was able to flex in the chordwise direction. The actuators were rubber muscle actuators (RMAs). When pressurized with air, the RMAs contract with a force generally proportional to the applied pressure. Similarly to hydraulic systems, these actuators require pneumatic systems, which typically have a weight penalty of the supporting hardware (compressor and accumulator, or pressure storage vessel, solenoids, control circuitry). The RMAs were connected to the leading and trailing edges of the wing; hence the contraction would cause an increase in camber. Two generations of prototypes were described with significant improvements made on the second generation. A very simple morphing wing was fabricated in phase one: the nose was able to elastically camber down by about 25° and the tail by 20°. The second generation wing fabrication methodology showed smooth elastic cambering and no buckling or waviness in the skins. In this case, the LE and the TE achieved 23° and 15° deflections respectively.

Bubert *et al* (2010) developed a passive elastomeric matrix composite morphing skin. They evaluated several elastomers, composite arrangements, and substructure configurations, leading to the selection of the most appropriate components for prototype development.

Popov *et al* (2008) presented an adaptive wing concept with an upper surface that deflected under single-point control. The flexible skin was placed at the laminar–turbulent boundary layer transition point, and different functions were tested to find whether the transition could be shifted towards the trailing edge and whether the drag could be reduced. In addition to static deflections, sinusoidal deflections were evaluated.

Abdullah *et al* (2009) used shape memory alloys to alter the shape of an airfoil to increase the L/D ratio throughout the flight regime of a UAV. A flexible skin was also utilized for variable camber control. The aerodynamic effect of camber location and magnitude was analyzed using a 2D panel-method. The researchers found that shifting the location of maximum camber thickness from 10% to 50% of the chord, and increasing the camber from 1% to 5%, maximized L/D for low angles of attack. Ideally, the wing would use this range to accommodate multiple flight conditions. The objective was predominantly cruise efficiency rather than control, and hence the response time of the SMA was considered to be acceptable.

Barbarino *et al* (2009a) investigated an active wing (via SMAs) that deformed its shape to provide a bumped wing geometry. This variation in the wing thickness is advantageous for transonic flight, but also has benefits in subsonic flight. Bench top experiments validated the efficacy of the concept. Barbarino *et al* (2007, 2008, 2009b) introduced several morphing trailing edge architectures to replace a conventional flap device. A compliant rib structure was designed, based on SMA actuators exhibiting structural potential (i.e. bearing the external aerodynamic loads). Numerical results, achieved through an FE approach, were presented in terms of trailing edge-induced displacement and morphed shape. Barbarino *et al* (2010) proposed a flap architecture for a variable camber trailing edge, whose reference geometry was based on a full scale wing for a regional transport aircraft. The compliant rib was based on a truss-like structure where some members were active rods made of SMA. The layout of the structure was obtained using a preliminary optimization process, incorporating practical constraints, by focusing on a basic truss-like element and its repetition and position within the overall truss. The structural performance was estimated using FE analysis. The SMA behavior was modeled using a dedicated routine to evaluate the internal stress state and the minimum activation temperature. The design fulfilled a number of key requirements: a smooth actuation along the chord; morphed shapes that assure the optimal aerodynamic load distribution for high lift; light weight; and low mechanical complexity. The design features of the architecture were investigated, and the requirements of the morphing skin discussed.

Icardi and Ferrero (2009) designed morphing wings with SMA torsion tubes and independent SMA wires for wing camber control. Their analysis delivered stress–strain curves for various types of SMA wires and stresses on structural wing components of the indicated design, including a supporting wing box section and surface material. Their theoretical model predicted that for a 1000 kg UAV with 1.2 m (mean) chord and 3 m span, the camber varied from 5° to 15.5° with SMA torsion tubes delivering 150 to 200 N m and drawing 1.2 kW of power.

5.3. SMA actuation bandwidth

The requirements for actuator speed and bandwidth strongly depend on the application/functionality of the morphing system. Morphing for performance enhancement allows more flexibility in the design of the actuator, while morphing for control authority sets many constraints on the design of the actuator in terms of speed, stroke, bandwidth and fatigue life. As discussed in this article, SMAs are mainly used for twist and camber morphing, hence mainly for control authority. Therefore, it is vital to consider various measures to improve the actuator design to achieve the desired response.

The main limiting factor for SMA actuation speed is thermal inertia. The martensitic thermo-plastic phase transformation can occur fairly quickly (0.1–5 Hz) and its speed is driven by the temperature change. Therefore, fast methods for both heating and cooling the alloy must be adopted to achieve quick cyclic actuation. Conventional methods for heating and cooling of SMAs involve resistive Joule heating and natural convection, respectively. Usually an increase in the amount of electric current used to heat the SMA actuator by resistive Joule heating produces reduced activation times (at the expense of more power). Cooling is usually slower than heating and deserves particular consideration to improve the overall cyclic response. Other methods could include bleeding hot air from engines for heating, which is a heavy and complex solution, or the use of forced air for cooling for air borne applications. Other applications could make use of existing on-board hot/cold fluids as a source/sink for thermal exchange.

In the literature, various methods have been developed to speed up SMA actuators. Many of these methods are initiated from robotic applications and include optimizing the heating of the alloy and/or improving the cooling process.

Featherstone and Teh Harn (2006) investigated a method to improve the speed of an SMA actuator for a robot by increasing the rate at which the SMA element can safely be heated. Their method consisted of measuring the electrical resistance of an SMA element, calculating a maximum safe heating current as a function of measured resistance, and ensuring that the actual heating current did not exceed this maximum value. They performed an experimental validation by incorporating their method into a two-stage relay controller that controlled the motion of a pantograph robot actuated by two antagonistic pairs of SMA wires. This resulted in a substantial increase in the maximum velocity attainable by this robot, without any change in the cooling regime, purely as a result of faster heating.

Similarly, Velazquez and Pissaloux (2012) investigated the thermal behavior of SMAs, in particular NiTi, and presented a comparative theoretical study of the performance of several temperature controllers to improve their actuation speed. They compared the performance of linear controllers to improve the heating process. To prevent overheating and thermal fatigue, the controllers accounted for the maximum heating current at which NiTi wires can safely be heated. They showed that a feed-forward controller can significantly improve the thermal dynamics of SMAs.

Seldon *et al* (2005) proposed a hysteresis loop control (HCL) method, specifying intermediate temperatures to be 'pulled back' to after extreme temperatures of cooling and heating had been reached. This methodology is claimed to have shortened latency times significantly and saved power. The actuation speed achieved by four segment coordination was 0.1 Hz. However, their overall design was heavy and bulky, resulting in very low engineering prospects. On the other hand, Siong Loh *et al* (2006) described a simple heat sink consisting of silicone grease and an outer metal tube. They verified the effectiveness of this heat sink using FEM analysis and experiments. They used a high current pulse actuation method and coupled with temperature control a response of 2.0 Hz and 1.70 mm oscillation amplitude was achieved.

Granito (2010) focused on improving the cooling process by using Peltier cells for both heating and cooling of SMAs. This study used the thermoelectric effect (direct conversion of temperature differences to electric voltage, and vice versa) of small heat pumps based on semiconductors to affect the temperature of an SMA ribbon. Thermal paste was used at the interface between the SMA ribbon and the Peltier cell. Both numerical analysis and experimental tests confirmed reductions in cooling time when compared to natural convection. In addition, the author claims to have reduced the overall energy consumption when comparing this method with a conventional resistive heating method.

Some manufacturers have also tried to improve the cooling process by coating the SMA actuator. Saes Getters (2013), for instance, produces and sells SMA wires with a silicone sleeve that has been tested to be ten times more effective than natural convection for cooling, as reported in table 4.

Table 4. Different cooling methods for SMAs and performance (Saes Getters 2013, Jani*et al* 2014, Dynalloy Inc. 2007).

	Speed performance increase
Increasing stress	1.2:1
Standard air convection	1:1
Solid heat sink materials	2:1
Higuer temperature wire	2:1
Forced air	4:1
Heat conductive grease	8:1
Silicon	10:1
Oil immersion	25:1
Water with glycol	100:1

5.4. Reduction of power consumption with SMAs

The need to reduce the overall power consumption is essential to maintain the system-level benefits of the morphing technology. One potential solution to reduce power consumption is to integrate the SMA actuator within multi-stable structures. The actuator will trigger the snap through of the structure from one stable position to another. Once the structure is in the new stable position, there is no need for the SMA actuator to keep working to maintain the deformation of the structure in the desired position. The stable position effectively works as a locking mechanism. The combination of an SMA actuator with a multi-stable structure produces an additional benefit related to strain/motion amplification. The limited amount of strain recovery of the SMA actuator (usually 3–4% of the initial length) is used to command the switching within the multi-stable structure from one stable position to another. This motion produces relatively large overall displacements, which is extremely welcome in morphing applications. In doing so, the low recovery strain of the SMA actuator also favorably affects its actuation cycles with stable performance and thus the overall fatigue life. There are few examples in the literature where SMA has been integrated with multi-stable structures.

Hufenbach *et al* (2002) adopted a novel adaptive structure of cylindrical shape consisting of GFRP bi-stable laminates with embedded SMA wires. The adaptive structure was integrated with an electrical circuit to initiate the snap through. The concept is promising as it does not require continuous power supply to maintain the desired shape.

Johnson *et al* (2010) examined the bi-stable behavior of an elastic arch to effectively extend the chord of a helicopter rotor blade. In this study the arch was clamped at both ends and an SMA wire was connected to the ends and the middle of the arch to induce the transition from one stable position to the other. Much effort was devoted to the design of flexures to avoid high strains leading to failure when the arch transitioned from one stable equilibrium condition to the other. In addition, the elastic arch was only actuated in one direction. These limitations were overcome in subsequent studies by Barbarino *et al* (2013) and Barbarino and Gandhi (2014). A bi-stable von Mises truss was used in place of the arch and two integrated SMA wires provided the actuation force to transition the von Mises truss from one stable equilibrium condition to the other, and back. In detail, one SMA wire was resistively heated to

drive the von Mises truss beyond the unstable equilibrium state and the other would be passively pre-stressed by the motion of the von Mises truss towards the second stable equilibrium. The two wires would then switch roles in moving the von Mises truss back from the second to the first stable equilibrium state, thus achieving two-way actuation. The authors modeled the combined behavior of the overall system and found good agreement with test data from an experimental prototype.

Dano and Hyer (2003) explored the use of SMA wires to change the equilibrium configuration of unsymmetric laminates. They developed an approximate theory to predict the snap through of unsymmetric laminates induced by SMA wires. The equations governing the laminate behavior were coupled to the equations governing the SMA wire behavior. Then, they used experiments to calibrate the model and to study SMA-induced deformations in four unsymmetric laminates.

Kim *et al* (2010) investigated SMAs combined with piezoelectric active structures to achieve reversible state changes for a bi-stable cantilever beam. The piezoelectric was used to induce a rapid change from state I to II which also deformed an attached SMA wire. This allowed resetting of the bi-stablity of the cantilever beam with a higher degree of controllability.

Another approach to power consumption reduction is to combine active, resistive heating of SMA actuators with passive, environmental temperature changes due to normal operation. In a similar approach, passive activation is sufficient for most cases and does not require any power. Active heating is used when supplementary control is necessary or when passive actuation is insufficient. The possibility of using passive systems has been discussed by Turner *et al* (2006) in the design of a novel adaptive engine chevron concept. Passive environmental heating has also been suggested by Mabe (2005) in the design of a hinge apparatus with a two-way controllable SMA hinge pin actuator.

An example application could be aircraft morphing flaps adopted for landing or take-off and implementing SMA technology for actuation. During normal operation, the temperature gradient between ground and cruise altitude (in excess of 70 °C in a typical mission profile, inversely dependent on altitude) would be sufficient to induce phase transition from martensite to austenite for SMA actuators. The environmental activation could also be used to only partially activate the flaps, for instance during take-off, while the supplemental powered activation could be provided during landing or when landing in particularly low-temperature conditions. Several strategies could be envisioned to optimize performance or power reduction, and must be tailored to the specific morphing application.

6. Conclusions

In this review, the main characteristics of shape memory alloys were discussed. SMAs are a unique class of metallic materials with the ability to recover their original shape at certain characteristic temperatures (shape memory effect) or to undergo large strains without plastic deformation or failure (super-elasticity). The fatigue behavior of SMAs was also reviewed, along with some studies carried out to study fatigue life.

A review of the state-of-the-art constitutive models was presented. It can be concluded that each model addresses specific loading conditions and presents limitations. In fact, no general model exists to date for SMAs. Theoretical and experimental investigations are still ongoing on this matter. The lack of a general model for shape memory alloys has limited the interest from aerospace companies.

Shape memory alloys have been used in a wide variety of applications in different fields. In this work, we focused on morphing aircraft, which represents the main contribution of the present article. This specific application of SMAs is particularly challenging due to the designer's effort in developing novel configurations which can maximize the integration and effectiveness of SMAs, which play the role of actuators (using the shape memory effect), often combined with structural, load-carrying capabilities. Iterative and multi-disciplinary modeling is therefore necessary due to the fluid–structure interaction combined with the nonlinear thermo-mechanical behavior of SMAs. Many structural configurations developed to date for morphing applications use simple SMA wires or rods. Often in-house tools are created to analyze and design the specific application.

Conventional heat exchange mechanisms of resistive heating and convection cooling are slow, resulting in a slow frequency response for SMA actuators. In most applications where a low temperature thermal sink is not available, SMAs are typically employed with relatively complex mechanical components (such as active fluidic cooling systems) to speed up their thermodynamic behavior.

Most of the studies that have used SMA for twist morphing are both numerical and experimental; however, flying test beds have not been achieved. The applications of SMAs are mainly for fighter aircraft and helicopters (and tiltrotors). For fighter aircraft, the use of SMAs is mainly to enhance the roll control authority. However, state-of-the-art SMA actuators fail to deliver the actuation rate required for fighter aircraft due to the high requirements in terms of agility and maneuverability. In contrast, SMAs seem to be a more promising technology for rotary wing aircraft (helicopters and tiltrotors) of different scales.

For camber morphing, the applications of SMAs vary between fighter aircraft, transport aircraft and UAVs, for both fixed wing and rotary wing configurations. Almost all of the research employs theoretical analysis, whereas only half employs experimental (benchtop) validation. Only one flight test has been achieved, where the application was a rotary wing UAV. Research has been directed mostly towards fixed wing applications since 2003.

In order to maintain the system-level benefits of the morphing technology, reduction of the overall power consumption is essential. One possible solution to achieve this reduction is the integration of SMA actuators within multi-stable structures, or the combination of active, resistive heating of SMA actuators with passive, environmental temperature changes due to normal operation.

Acknowledgments

EI Saavedra Flores acknowledges support from Department of Civil Engineering, University of Santiago, Chile, and also from the National Commission for Scientific and Technological Research (CONICYT), from the Chilean government. I Dayyani and MI Friswell acknowledge the support of the European Research Council through project 247045 entitled 'Optimisation of Multi-scale Structures with Applications to Morphing Aircraft'.

References

Abdullah E J, Bill C and Watkins S 2009 Application of smart materials for adaptive airfoil control *47th AIAA Aerospace Sciences Meeting Including the New Horizons Forum and Aerospace Exposition (Orlando, FL)* AIAA 2009-1359

Alasty A, Alemohammad S H, Khiabani R H and Khalighi Y 2004 Maneuverability improvement for an ultra light airplane model using variable shape wing *AIAA Atmospheric Flight Mechanics Conf. and Exhibit (Providence, RI)* AIAA 2004-4831

Arbogast D J, Ruggeri R T and Bussom R C 2008 Development of a 1/4-scale NiTinol actuator for reconfigurable structures *Proc. SPIE* **6930** 69300L

Arghavani J, Auricchio F, Naghdabadi R, Reali R and Sohrabpour S 2010 A 3-D phenomenological constitutive model for shape memory alloys under multiaxial loadings *Int. J. Plasticity* **26** 976–91

Auricchio F, Coda A, Reali A and Urbano M 2009 SMA numerical modeling versus experimental results: parameter identification and model prediction capabilities *J. Mater. Eng. Perform.* **18** 649–54

Auricchio F, Mielke A and Stefanelli U 2008 A rate-independent model for the isothermal quasi-static evolution of shape-memory materials *Math. Models Methods Appl. Sci.* **18** 125–64

Auricchio F and Reali A 2008 Shape memory alloys: material modeling and device finite element simulations *Mater. Sci. Forum* **583** 257–75

Auricchio F, Reali A and Stefanelli U 2007 A three-dimensional model describing stress-induced solid phase transformation with permanent inelasticity *Int. J. Plasticity* **23** 207–26

Barbarino S 2009 Smart morphing concepts and applications for advanced lifting surfaces *PhD Thesis* University of Napoli 'Federico II', Napoli, Italy

Barbarino S, Ameduri S, Lecce L and Concilio A 2009a Wing shape control through an SMA-based device *J. Intell. Mater. Syst. Struct.* **20** 283–96

Barbarino S, Ameduri S and Pecora R 2007 Wing camber control architectures based on SMA: numerical investigations *SPIE* **6423**

Barbarino S, Bilgen O, Ajaj R M, Friswell M I and Inman D J 2011 A review of morphing aircraft *J. Intell. Mater. Syst. Struct.* **22** 823–77

Barbarino S, Concilio A, Pecora R, Ameduri S and Lecce L 2008 Design of an actuation architecture based on SMA technology for wing shape control *Actuator 2008 Conf. (Bremen)* P144

Barbarino S, Dettmer W G and Friswell M I 2010 Morphing trailing edges with shape memory alloy rods *ICAST: 21st Int. Conf. on Adaptive Struct. Technol. (State College, PA)*

Barbarino S and Gandhi F 2014 A cellular frame for morphing applications based on Bi-stable von-Mises Trusses actuated using shape memory alloys *Proc. 22nd AIAA/ASME/AHS Adaptive Struct. Conf. (National Harbor, MD, Jan. 2014)*

Barbarino S, Gandhi F and Visdeloup R A 2013 Bi-stable von-Mises truss for morphing applications actuated using shape memory alloys *Proc. ASME 2013 Conf. on Smart Materials, Adaptive Structures and Intelligent Systems (Snowbird, UT, Sept. 2013)*

Barbarino S, Pecora R, Lecce L, Concilio A, Ameduri S and Calvi E 2009b A novel SMA-based concept for airfoil structural morphing *J. Mater. Eng. Perf.* **18** 696–705

Barrett R M, Burger C and Melian J P 2001 Recent advances in uninhabited aerial vehicle (UAV) flight control with adaptive aerostructures *4th European Demonstrators Conf. (Edinburgh)*

Beauchamp C H and Nedderman W H Jr 2001 Controllable camber windmill blades *US Patent* US6465902

Benavides J C and Correa G 2004 *Morphing Wing Design Using Nitinol Wire* (Rolla, MO: Intelligent System Center, University of Missouri-Rolla)

Bertacchini O, Lagoudas D and Patoor E 2003 Fatigue life characterization of shape memory alloys undergoing thermomechanical cyclic loading *Proc. SPIE* **5053** 612–24

Boyd J G and Lagoudas D C 1996a A thermodynamical constitutive model for shape memory materials: Part I. The monolithic shape memory alloys *Int. J. Plasticity* **12** 805–42

Boyd J G and Lagoudas D C 1996b A thermodynamical constitutive model for shape memory materials: Part II. The monolithic shape memory alloys *Int. J. Plasticity* **12** 843–73

Brailovski V, Terriault P, Coutu D, Georges T, Morellon E, Fischer C and Bérubé S 2008 Morphing laminar wing with flexible extrados powered by shape memory alloy actuators *SMAS 2008: Int. Conf. on Smart Materials, Adaptive Structures and Intelligent Systems (Ellicott City, MD)* SMASIS2008-377

Brinson L C 1990 One-dimensional constitutive behaviour of shape memory alloy constitutive models *J. Intell. Mater. Syst. Struct.* **1** 207–34

Brocca M, Brinson L C and Bazant Z P 2002 Three dimensional constitutive model for shape memory alloys based on microplane model *J. Mech. Phys. Solids* **50** 1051–77

Bubert E A, Woods B K S, Kothera C and Wereley N M 2010 Design and fabrication of a passive 1-D morphing skin *J. Intell. Mater. Syst. Struct.* **21** 1697–8

Buehler W J, Gilfrich J V and Wiley R C 1963 Effect of low-temperature phase changes on the mechanical properties of alloys near composition TiNi *J. Appl. Phys.* **34** 1475

Buehler W J, Wiley R C and Wang F E 1965 Nickel-based alloys *US Patent Specification* 317485123

Bushnell G S, Arbogast D J and Ruggeri R T 2008 Shape control of a morphing structure (rotor blade) using a shape memory alloy actuator system: future of SMA *Proc. SPIE* **6928** 69282A

Calkins F T, Mabe J H and Ruggeri R T 2008 Overview of Boeing's shape memory alloy based morphing aerostructures *SMASIS 2008: Proc. ASME Conf. on Smart Materials, Adaptive Structures and Intelligent Systems (Ellicott City, MD)* SMASIS2008-648

Chandra R 2001 Active shape control of composite blades using shape memory actuation *Smart Mater. Struct.* **10** 1018–24

Chang L C and Read T A 1951 Plastic deformation and diffusionless phase changes in metals—the gold–cadmium beta phase *Trans. AIME* **189** 47–52

Chang B-C, Shaw J A and Iadicola M A 2006 Thermodynamics of shape memory alloy wire: modeling, experiments, and application *Continuum Mech. Thermodyn.* **18** 83–118

Chemisky Y, Duval A, Patoor E and Zineb T B 2011 Constitutive model for shape memory alloys including phase transformation, martensitic reorientation and twins accommodation *Mech. Mater.* **43** 361–76

Chemisky Y, Duval A, Piotrowski B, Ben-Zineb T and Patoor E 2008 Numerical tool based on finite element method for SMA structures design *SMASIS: Proc. ASME 2008 Conf. on Smart Mater., Adaptative Struct. & Intell. Syst. (Turf Valley Resort, Ellicott City, MD, Oct.)* SMASIS08-485

Chopra I 2001 *Recent Progress on Development of a Smart Rotor System* (Langley, VA: NASA Langley Research Center)
Chopra I 2002 Review of state of art of smart structures and integrated systems *AIAA J.* **40** 2145–87
Collet M 2008 Modeling implementation of smart materials such as shape memory alloys and electro-active metamaterials *Proc. COMSOL Conf. 2008 (Hannover)*
Cong D Y, Zhang Y D, Wang Y D, Humbert M, Zhao X, Watanabe T, Zuo L and Esling C 2007 Experiment and theoretical prediction of martensitic transformation crystallography in a Ni–Mn–Ga ferromagnetic shape memory alloy *Acta Mater.* **55** 4731–40
Dano M L and Hyer M W 2003 SMA-induced snap-through of unsymmetric fibre-reinforced composite laminates *Int. J. Solids Struct.* **40** 5949–72
Duerig T W and Pelton A R 1994 *Ti–Ni Shape Memory Alloys, Materials Properties Handbook, Titanium Alloys* (Ohio: ASM International)
Dynalloy Inc. 2007 *Technical Characteristics of Flexinol Actuator Wires* (Costa Mesa, CA: Dynalloy) p 12
Eggeler G, Hornbogen E, Yawny A, Heckmann A and Wagner M 2004 Structural and functional fatigue of NiTi shape memory alloys *Mater. Sci. Eng.* A **378** 24–33
Elahinia M H and Ahmadian M 2005a An enhanced SMA phenomenological model: I. The shortcomings of the existing models *Smart Mater. Struct.* **14** 1297–308
Elahinia M H and Ahmadian M 2005b An enhanced SMA phenomenological model: II. The experimental study *Smart Mater. Struct.* **14** 1309–19
Elzey D M, Sofla A Y N and Wadley H N G 2003 A bio-inspired, high-authority actuator for shape morphing structures *Proc. SPIE* **5053** 92
Epps J J and Chopra I 2001 In-flight tracking of helicopter rotor blades using shape memory alloy actuators *Smart Mater. Struct.* **10** 104–11
Fabrizio M and Pecoraro M 2013 Phase transitions and thermodynamics for the shape memory alloy AuZn *Meccanica* **48** 1695–700
Featherstone R and Teh Harn Y 2006 Improving the speed of shape memory alloy actuators by faster electrical heating *Spring Tracts Adv. Robot.* **21** 67–76
Frenzel J, George E P, Dlouhy A, Somsen Ch, Wagner M F-X and Eggeler G 2010 Influence of Ni on martensitic phase transformations in NiTi shape memory alloys *Acta Mater.* **58** 3444–58
Fugazza D 2005 Experimental investigation on the cyclic properties of superelastic NiTi shape-memory alloy wires and bars *PhD Thesis* University of Pavia, Italy
Gall K, Tybera J, Wilke ersa G, Robertsonb S W, Ritchieb R O and Maier H J 2008 Effect of microstructure on the fatigue of hot-rolled and cold-drawn NiTi shape memory alloys *Mater. Sci. Eng.* A **486** 389–403
Gerstner E 2002 Shape-memory alloys www.nature.com/materials/news/features/021003/portal/m021003-6.html (last accessed: March 2014)
Gong X-Y, Pelton A R, Duerig T W, Rebelo N and Perry K 2004 Finite element analysis and experimental evaluation of superleastic nitinol stent *SMST-03: Proc. Int. Conf. on Shape Memory and Superleastic Technologies (Pacific Grove, CA, May)* ed A R Pelton and T W Duerig pp 443–51
Granito M 2010 A cooling system for shape memory alloy based on the use of Peltier cells *PhD Thesis* University of Naples 'Federico II', Italy
Greninger A B and Mooradian V G 1938 Strain transformation in metastable beta copper–zinc and beta copper–tin alloys *Trans. AIME* **128** 337–68
Haag C, Tandale M and Valasek J 2005 Characterization of shape memory alloy behavior and position control using reinforcement learning *Proc. AIAA Infotech@Aerospace Conf. (Arlington, VA, Sept.)* 2005-7160
Han L H and Lu T J 2006 3D finite element simulation for shape memory alloys *IUTAM Symp. Mechanics and Reliability of Actuating Materials* ed W Yang pp 227–36
He Y J and Sun Q P 2011 Rate-dependent damping capacity of NiTi shape memory alloy *Solid State Phenom.* **172–174** 37–42
Heintze O 2004 A computationally efficient free energy model for shape memory alloys—experiments and theory *PhD Thesis* University of North Carolina
Hodgson D E, Wu M H and Biemann R J 1990 *Shape Memory Alloys, Metals Handbook* vol 2 (Ohio: ASM International) pp 897–902
Huan W 1998 Shape memory alloys and their application to actuators for deployable structures *PhD Thesis* Cambridge University
Huang W 2002 On the selection of shape memory alloys for actuators *Mater. Des.* **23** 11–9
Huang W and Toh W 2000 Training two-way shape memory alloy by reheat treatment *J. Mater. Sci. Lett.* **19** 1549–50
Hufenbach W, Gude M and Kroll L 2002 Design of multistable composites for application in adaptive structures *Comput. Sci. Technol.* **62** 2201–7
Icardi U and Ferrero L 2009 Preliminary study of an adaptive wing with shape memory alloy torsion actuators *Mater. Des.* **30** 4200–10
Ivshin Y and Pence T J 1994 A thermo mechanical model for one variant shape memory material *J. Intell. Mater. Syst. Struct.* **5** 455–73
Jackson C M, Wagner H J and Wasilewski R J 1972 55-Nitinol—the alloy with a memory: its physical metallurgy, properties, and applications *Report* NASA SP-5110
Jani J M, Leary M, Subic A and Gibson M A 2014 A review of shape memory alloy research, applications and opportunities *Mater. Des.* **56** 1078–113
Johnson Matthey Inc. 2013 http://www.jmmedical.com/ (last accessed: 26 February 2013)
Johnson T, Gandhi F and Frecker M 2010 Modeling and experimental validation of a bistable mechanism for chord extension morphing rotors *Proc. SPIE* **7643** 76432B
Kadkhodaei M, Rajapakse R K N D, Mahzoon M and Salimi M 2007a Modeling of the cyclic thermomechanical response of SMA wires at different strain rates *Smart Mater. Struct.* **16** 2091–101
Kadkhodaei M, Salimi M, Rajapakse R K N D and Mahzoon M 2007b Microplane modeling of shape memory alloys *Phys. Scr.* **T129** 329–34
Kadkhodaei M, Salimi M, Rajapakse R K N D and Mahzoon M 2008 Modeling of shape memory alloys based on microplane theory *J. Intell. Mater. Syst. Struct.* **19** 541–50
Kan Q and Kang G 2010 Constitutive model for uniaxial transformation ratchetting of super-elastic NiTi shape memory alloy at room temperature *Int. J. Plasticity* **26** 441–65
Kauffman G B and Mayo I 1993 The metal with a memory *Invent. Technol.* **9** 18–23
Kim H A, Betts D N, Salo A I T and Bowen C R 2010 Shape memory alloy-piezoelectric active structures for reversible actuation of bistable compoistes *AIAA J.* **48** 1265–8
Kirkpatrick K and Valasek J 2008 Reinforcement learning for active length control of shape memory alloys *AIAA Guidance, Navigation and Control Conf. and Exhibit (Honolulu, Hawaii, Aug.)* 2008-7280
Kudva J N 2001 Overview of the DARPA/AFRL/NASA smart wing phase II program *Smart Structures and Materials Conf.* pp 383–9
Kudva J N 2004 Overview of the DARPA smart wing project *J. Intell. Mater. Syst. Struct.* **15** 261–7

Kudva J N and Carpenter B 2000 Smart Wing Program *DARPA Technology Interchange Meeting (June 2000)*
Kudva J N, Jardine P, Martin C and Appa K 1996a Overview of the ARPA/WL 'Smart Structures and Material Development—Smart Wing' contract *Proc. SPIE* **2721** 10
Kudva J N, Lockyer A J and Appa K 1996b Adaptive aircraft wing *Smart Structures and Materials: Implications for Military Aircraft of New Generation* (*AGARD SMP Lecture Series* 205) 10-1
Kumar G 2000 Modeling and design of one dimensional shape memory alloy actuators *MSc Thesis* The Ohio State University, USA
Kumar P K and Lagoudas D C 2008 *Shape Memory Alloys: Modeling Engineering Applications* ed D C Lagoudas (Berlin: Springer)
Lexcellent C 2013 *Shape-Memory Alloys Handbook (Materials Science Series)* (Hoboken, NJ: ISTE/Wiley)
Lin R 1996 Shape memory alloys and their applications http://www.stanford.edu/~richlin1/sma/sma.html (last accessed 26 February 2013)
Li Q and Seelecke S 2007 Thermo-mechanically coupled analysis of shape memory actuators *Proc. COMSOL Users Conf. 2007 (Boston, MA)*
Liang C and Rogers C A 1990 One-dimensional thermomechanical constitutive relations for shape memory material *J. Intell. Mater. Syst. Struct.* **1** 207–34
Lin P H, Tobushi H, Ikai A and Tanaka K 1995 Deformation properties associated with the martensitic and R-phase transformations in TiNi shape memory alloy *J. Appl. Biomech.* **10** 1–11
Lv H, Leng J and Du S 2009 A survey of adaptive materials and structures research in China *50th AIAA/ASME/ASCE/ASH/ACS Structures, Structural Dynamics, and Materials Conf.* (*Palm Springs, CA*)
Mabe J 2005 Hinge apparatus with two-way controllable shape memory alloy (SMA) hinge pin actuator and methods of making two-way SMA parts *US Patent Specification* 10/796806
Madden J D W, Schmid B, Hechinger M, Lafontaine S R, Madden P G A and Hover F S 2004 Application of polypyrrole actuators: feasibility of variable camber foils *IEEE J. Ocean. Eng.* **29** 738–49
Mahmud A S, Liu Y and Nam T 2008 Gradient anneal of functionally graded NiTi *Smart Mater. Struct.* **17** 015031
Martin C A, Kudva J, Austin F, Jardine A P, Scherer L B, Lockyer A J and Carpenter B F 1998 Smart materials and structures—smart wing volumes I, II, III, and IV *Report* AFRL-ML-WP-TR-1999-4162
Matheus T C U, Menezes W M M, Rigo O D, Kabayama L K, Viana C S C and Otubo J 2011 The influence of carbon content on cyclic fatigue of NiTi SMA wires *Int. Endodontic J.* **44** 567–73
Matsuzaki Y, Naito H, Ikeda T and Funami K 2001 Thermo-mechanical behaviour associated with pseudoelastic transformation of shape memory alloys *Smart Mater. Struct.* **10** 884–92
Mehrabi R and Kadkhodaei M 2013 3D phenomenological constitutive modeling of shape memory alloys based on microplane theory *Smart Mater. Struct.* **22** 025017
Miller D A 2003 Thermomechanical characterization of plastic deformation and tranformation fatigue in shape memory alloys *PhD Thesis* Texas A&M University
Miller D A and Lagoudas D C 2000 Thermo-mechanical characterization of NiTiCu and NiTi SMA actuators: influence of plastic strains *Smart Mater. Struct.* **9** 640–52
Mirone G 2007 Design and demonstrators testing of adaptive airfoils and hingeless wings actuated by shape memory alloy wires *Smart Struct. Syst.* **3** 89–114
Mirone G and Pellegrino A 2009 Prototipo di sezione alare adattiva per UAV: centina deformabile con attuatori in SMA *AIAS: 38th Proc. Convegno Nazionale, Associazione Italiana per l'Analisi delle Sollecitazioni (Turin, Sept. 2009)* (in Italian)
Morin C, Moumni Z and Zaki W 2011 A constitutive model for shape memory alloys accounting for thermomechanical coupling *Int. J. Plasticity* **27** 748–67
Naito H, Matsuzaki Y and Ikeda T 2001 A unified model of thermo-mechanical behaviour of shape memory alloys *Society of Photo-Optical Instrumentation Engineers* vol 4333 (Bellingham, WA: International Society for Optical Engineering) pp 291–313
Nam C, Chattopadhyay A and Kim Y 2002 Application of shape memory alloy (SMA) spars for aircraft maneuver enhancement *Proc. SPIE* **4701** 226
Ölander A Z 1932 *Kristal* **83(A)** 145
Otsuka K and Wayman C M 1998 *Shape Memory Materials* (Cambridge: Cambridge University Press)
Peel L D, Mejia J, Narvaez B, Thompson K and Lingala M 2008 Development of a simple morphing wing using elastomeric composites as skins and actuators *SMASIS 2008: ASME Conf. on Smart Materials, Adaptive Structures and Intelligent Systems (Ellicott City, MD)* SMASIS2008-544
Peel L D, Mejia J, Narvaez B, Thompson K and Lingala M 2009 Development of a simple morphing wing using elastomeric composites as skins and actuators *J. Mech. Des.* **131** 091003
Peng X, Li H and Chen W 2005 A comprehensive description for shape memory alloys with a two-phase mixture model incorporating the conventional theory of plasticity *Smart Mater. Struct.* **14** 425–33
Popov A V, Labib M, Fays J and Botez R M 2008 Closed-loop control simulations on a morphing wing *J. Aircraft* **45** 1794–803
Prahlad H and Chopra I 2001a Comparative evaluation of shape memory alloy constitutive models with experimental data *J. Intell. Mater. Syst. Struct.* **12** 386–96
Prahlad H and Chopra I 2001b Design of a variable twist tilt-rotor blade using shape memory alloy (SMA) actuators *Proc. SPIE* **4327** 46–59
Richter F, Kastner O and Eggeler G 2009 Implementation of the Müller-Achenbach-Seelecke model for shape memory alloys in ABAQUS *J. Mater. Eng. Perform.* **18** 626–30
Roglin R L, Hanagud S V and Kondor S 1994 Adaptive airfoils for helicopters *35th AIAA Structures, Structural Dynamics and Materials Conf. (Hilton Head, SC)*
Roglin R L and Hanagud S V 1996 A helicopter with adaptive rotor blades for collective control *Smart Mater. Struct.* **5** 76
Ruggeri R T, Arbogast D J and Bussom R C 2008 Wind tunnel testing of a lightweight 1/4-scale actuator utilizing shape memory alloy *49th AIAA/ASME/ASCE/AHS/ASC Structures, Structural Dynamics, and Materials Conf. (Schaumburg, IL)* 2008–2279
Saavedra Flores E I, Diaz Delao F A, Friswell M I and Sienz J 2012 A computational multi-scale approach for the stochastic mechanical response of foam-filled honeycomb cores *Comput. Struct.* **94** 1861–70
Saavedra Flores E I and Friswell M I 2012 Multi-scale finite element model for a new material inspired by the mechanics and structure of wood cell walls *J. Mech. Phys. Solids* **60** 1296–309
Saavedra Flores E I and Friswell M I 2013 Ultrastructural mechanisms of deformation and failure in wood under tension *Int. J. Solids Struct.* **50** 2050–60
Saeedvafa M 2002 A constitutive model for shape memory alloys *Internal MSC Report*
Saes Getters 2013 *SMA Products Datasheet* http://www.saesgetters.com/sites/default/files/SMA%20products%20datasheets_0.pdf (last accessed: December 2013)
Sanders B, Cowan D and Scherer L 2004 Aerodynamic performance of the smart wing control effectors *J. Intell. Mater. Syst. Struct.* **15** 293–303
Scirè Mammano G and Dragoni E 2011 Functional fatigue of shape memory wires under constant-stress and constant-strain loading conditions *Procedia Eng.* **10** 3692–707
Scirè Mammano G and Dragoni E 2013 Functional fatigue of NiTi shape memory wires for a range of end loadings and constraints *Frattura ed Integrita Strutturale* **23** 25–33

Seldon B, Cho K J and Asada H 2005 Multi segment state coordination for reducing latency time of shape memory alloy actuator system *Proc. 2005 IEEE ICRA* pp 1362–7
Shimizu K and Tadaki T 1987 *Shape Memory Alloys* ed H Funakubo (New York: Gordon and Breach) pp 1–60
Shrivastava S 2006 Simulation for thermomechanical behavior of shape memory alloy (SMA) using COMSOL multiphysics *Proc. COMSOL Users Conf. 2006 (Bangalore)*
Shuai S, Yen-Yu L and Xi L 2009 Fundamental characteristics of shape memory alloys http://smagroup.blogspot.com/2009/02/fundamental-characteristics-of-shape.html (last accessed: March 2014)
Singh K and Chopra I 2002 Design of an improved shape memory alloy actuator for rotor blade tracking *North American Symp. on Smart Structures and Materials* vol 4701 *(Society of Photo-Optical Instrumentation Engineers)* (Bellingham, WA: International Society for Optical Engineering) pp 244–66
Siong Loh C, Yokoi H and Arai T 2006 Natural heat-sinking control method for high-speed actuation of the SMA *Int. J. Adv. Robot. Sys.* **3** 303–12
Sittner P, Stalmans R and Tokuda M 2000 An algorithm for prediction of the hysteresis responses of shape memory alloys *Smart Mater. Struct.* **9** 452–65
Sofla A Y N, Elzey D M and Wadley H N G 2008 Two-way antagonistic shape actuation based on the one-way shape memory effect *J. Intell. Mater. Syst. Struct.* **19** 1017–27
Sreekumar M, Nagarajan T and Singaperumal M 2008 Modelling and simulation of a novel shape memory alloy actuated compliant parallel manipulator *J. Mech. Eng. Sci.* **222** 1049–59
Srinivasan A V and McFarland D M 1995 *Smart Structures: Analysis and Design* (Cambridge: Cambridge University Press)
Strelec J K, Lagoudas D C, Khan M A and Yen J 2003 Design and implementation of a shape memory alloy actuated reconfigurable airfoil *J. Intell. Mater. Syst. Struct.* **14** 257–73
Takeda K, Mitsui K, Tobushi H, Levintant-Zayonts N and Kucharski S 2013 Influence of nitrogen ion implantation on deformation and fatigue properties of TiNi shape memory alloy wire *Archiv. Mech.* **65** 391–405
Tanaka K 1986 A thermomechanical sketch of shape memory effect: one-dimensional tensile behaviour *Res. Mech.* **18** 251–63
Tanaka K, Nishimura F, Matsui H, Tobushi H and Lin P H 1996 Phenomenological analysis of plateaus on stress–strain hysteresis in TiNi shape memory alloy wires *Mech. Mater. Int. J.* **24** 19–30
Teh H Y 2008 Fast, accurate force and position control of shape memory alloy actuators *PhD Thesis* The Australian National University
Terriault P, Viens F and Brailovski V 2006 Non-isothermal finite element modeling of a shape memory alloy actuator using ANSYS *Comput. Mater. Sci.* **36** 397–410
Thiebaud F, Collet M, Foltete E and Lexcellent C 2005 Implementation of a multi-axial pseudoelastic model in FEMLAB to predict dynamical behaviour of shape memory alloys *Proc. COMSOL Conf. 2005 (Paris)*
Tobushi H, Hachisuka T, Yamada S and Lin P H 1997 Rotating-bending fatigue of a TiNi shape-memory alloy wire *Mech. Mater.* **26** 35–42
Tobushi H, Lin P H, Tanaka K, Lexcellent C and Ikai A 1995 Deformation properties of TiNi shape memory alloy *J. Physique* IV **5** 409–10
Tobushi H, Yamada S, Hachisuka T, Ikai A and Tanaka K 1996 Thermomechanical properties due to martensitic and R-phase transformations of TiNi shape memory alloy subjected to cyclic loadings *Smart Mater. Struct.* **5** 788–95
Turner T L, Buehrle R D, Cano R J and Fleming G A 2006 Modeling, fabrication, and testing of a SMA hybrid composite jet engine chevron concept *J. Intell. Mater. Syst. Struct.* **17** 483–97
Valasek J, Doebbler J, Tandale M and Meade A J 2008 Improved adaptive-reinforcement learning control for morphing unmanned air vehicles *IEEE Trans. Systems Man Cybern.* B **38** 1014–20
Valasek J, Tandale M and Rong J 2005 A reinforcement learning—adaptive control architecture for morphing *J. Aerospace Comput. Inf. Commun.* **2** 174–95
Velazquez R and Pissaloux E E 2012 Modelling and temperature control of shape memory alloys with fast electric heating *Int. J. Mech. Control* **13** 1–8
Vocke R D III, Kothera C S, Woods B K S, Bubert E A and Wereley N M 2012 One dimensional morphing structures for advanced aircraft *Recent Adv. Aircraft Technol.* (Vienna: InTech Publishers) chapter 1, pp 3–28
Vocke R D III, Kothera C S, Woods B K S and Wereley N M 2011 Development and testing of a span-extending morphing wing *J. Intell. Mater. Syst. Struct.* **22** 879–90
Wada K and Liu Y 2006 Some factors affecting the shape recovery properties of NiTi SMA *47th AIAA/ASME/ASCE/AHS/ASC Structures, Structural Dynamics, and Materials Conf. (Newport, RI, May)* 2006-1969
Yang S and Seelecke S 2008 Modeling and analysis of SMA-based adaptive structures *Proc. COMSOL Conf. 2008 (Boston, MA)*
Yu C, Kang G, Kan Q and Song D 2013 A micromechanical constitutive model based on crystal plasticity for thermo-mechanical cyclic deformation of NiTi shape memory alloys *Int. J. Plasticity* **44** 161–91
Yu H J, Wang Z G, Zu X T, Yang S Z and Wang L M 2006 Temperature memory effect in two-way shape memory TiNi and TiNiCu springs *J. Mater. Sci.* **41** 3435–9
Zaki W and Moumni Z 2007 A three-dimensional model of the thermomechanical behavior of shape memory alloys *J. Mech. Phys. Solids* **55** 2455–90